Trans. JWRI, Vol. 25(1996), No.2

Computational Welding Mechanics and Its Interface with Industrial Application

by **Hidekazu Murakawa**

Joining and Welding Research Institute, Osaka Universit
Ibaraki, Osaka, Japan

Abstract

The welding involves various physical phenomena, such as heat generation, heat and mass flow, melting and solidification, phase transportation and generation of residual stresses and distortions. Among theses, mathematical and numerical bases for the theoretical prediction of the mechanical phenomena are relatively well established However, the theoretical predictions using the finite element method, for example, is not widely accepted in assembly lines or construction sites. In this report, potential usefulness of the computational welding mechanics is demonstrated through various examples.

1. Introduction

In this report, practical application of computational welding mechanics is discussed. The first milestone in the computational welding mechanics is the theoretical establishment of the Finite Element Method (FEM) based on the thermal-elastic-plastic (T.E.P.) theory[1, 2]. Since then, theoretical model for the welding has been advanced by introducing various phenomena, such as creep, phase transformation and full coupling among material, temperature and mechanical fields. Also, the rapid advances of the computing facilities must be mentioned. Now, three dimensional simulation of practical welding problem can be solved on a personal computer. The computed results can be displayed in wonderful color three dimensional graphics.

Then, we must ask ourselves, "Is the computational welding mechanics truly attractive for people in industries now?". Figuratively speaking, it is like a human being. A man or a woman must have strong bones, brain, mussels, skin and wear decent clothes. The bones or the framework may correspond to the mathematical representation of physical phenomena. The mussels correspond to numerical methods such as finite element methods and finite difference methods. The brain is a computer or a system of computers. The skin and the clothes may be regarded as the computer graphic technology for pre/post processings. In addition to these, the most important thing in judging the attractiveness is what he or she does. In other words, whether the computational welding mechanics is useful for industries?

The computational mechanics, in general sense, is widely employed in researches and designs. But, the gap between the computer simulation and the welding in assembly lines or construction sites are extremely large. At the same time, it may be true that unrecognized but immediate needs for the theoretical prediction exist in these fields of the industries. Since all the fundamental elements, including easy access to computers, are available, now is the ideal time to introduce the computational welding mechanics into to assembly lines or construction sites.

Transactions of JWRI is published by Joining and Welding Research Institute of Osaka University, Ibaraki, Osaka567, Japan.

2. Various Aspects of Computational Welding Mechanics

From the aspect of modeling, the computational welding mechanics can be divided into four parts, namely,

(1) mathematical modeling of physical phenom ena
(2) numerical solution model
(3) conceptual modeling
(4) strategic modeling

The last two modelings are rather strange but very important to make the computational welding mechanics attractive. The conceptual modeling is the model which helps the understanding and the interpretation of the phenomena in a general and consistent manner. The strategic modeling is the overall planing which makes the research successful by integrating the mathematical modeling, numerical modeling and conceptual modeling. These four aspects of the modeling are discussed using the problems of welding and line heating as examples in chapters 4 and 5.

On the other hand, the process to be studied can be divided into the following stages, namely

(1) heat source (heat generation, heat flow)
(2) material (melting, solidification, phase transformation)
(3) mechanics (distortion, strain, stress)
(4) assessment (strength, elongation, fracture toughness)
(5) optimization of design and control (process control, material choice)

Thus, the computational mechanics must cover the whole scope from the heat source to the optimization of the welding process. In chapter 6, the spot welding is chosen as an example to demonstrate potential usefulness of the computational welding mechanics which covers a broad aspect of engineering problems.

3. FEM and Inherent Strain

3.1 Histories of computational welding mechanics

Important concepts in welding mechanics were established quite early based on the analytical investigations. N.S. Boulton[3], J.T. Norton, D. Rosenthal[4], T. Naka, T. Okumura[5], M. Otani[6], M. Watanabe, K. Satoh[7] and I. Tuji[8] were the pioneers in this field. The invention of the digital computers and the developments of numerical methods such as the Finite Element Methods during the 1970's made us possible to start new generation of welding mechanics. That is the computational welding mechanics. The problems solved in 1970's are rather simple. But, two dimensional problems under moving heat source were already studied. The FEM was soon applied to multi-pass welding problems.

One of the significant differences between the researches in the 1970-80's and these in the 90's is the scale and the precision of the models. Due to the great advance in the computer technology, large scale nonlinear transient problems can be solved on work stations. This makes it possible to analyze the real model rather than the scaled or simplified experimental model and gives special advantage to the computational mechanics compared to physical experiments. The advantages of computational welding mechanics over the experiments are,

(1) The size of the model and the welding conditions are not subjected to physical limitations of apparatus.
(2) Cost may be less than experiments.
(3) The information which is not physically measurable can be obtained.
(4) Ideal condition can be easily achieved. Thus, computational welding mechanics is effective to identify the influential factors.

3.2 Framework of thermal-elastic-plastic model

In general, mechanical behavior of elastic-plastic material under a thermal cycle can be described by,

(1) strain-displacement relation (compatibility condition)
(2) stress-strain relation (constitutive relation)
(3) equilibrium condition
(4) appropriate boundary conditions

Among these, the constitutive relation is the

most important in the welding mechanics. One of the fundamental assumption is that the total strain can be separated into the sum of the elastic, the plastic and the thermal strains, i.e.,

$$\varepsilon = \varepsilon^e + \varepsilon^p + \varepsilon^t \qquad (1)$$

where, ε, ε^e, ε^p and et are the total, the elastic, the plastic and the thermal strain, respectively.

3.3 Concept of inherent strain[9,10]

Since, the thermal strain disappears when the temperature returns to the room temperature after the thermal cycle, Eq.(1) becomes,

$$\varepsilon = \varepsilon^e + \varepsilon^p \qquad (2)$$

where the elastic strain ε^e is produced by the residual stress and the total strain ε corresponds to the residual deformation. By rewriting Eq.(2) as,

ε^*(inherent strain)= ε^p = ε^e(residual stress) -ε (residual deformation) (3)

it is seen, conceptually, that the residual stress and the residual deformation are produced by the inherent strain. In other words, the residual stress and the residual deformation can be determined when the inherent strain is known. In case of the thermal-elastic-plastic problem, the inherent strain is the residual plastic strain itself if there is no initial stress or initial gap in geometry.

When the problem involves phenomena, such as creep and phase transformation, creep strain and volumetric change due to the transformation can be included in Eqs.(1) and (3) as a part of the inelastic strain and the inherent strain.

3.4 Inherent strain in computational welding mechanics

The distortion and the residual stress due to thermal processes, such as cutting, bending and welding, are very important to ensure the geometrical precision and the mechanical strength and reliability. As it is discussed in the preceding section, both the distortion and the residual stress are produced by inherent strain. Thus, the inherent strain can be a conceptual backbone for the consistent understanding of the phenomena and the better usage of the computational method. Though it is a powerful tool, the Finite Element Method alone is just a numerical method. When the concept of inherent strain is combined with the FEM, the computational welding mechanics becomes truly attractive and useful.

The concept of inherent strain is very useful in the following aspects;

(1) It helps the understanding of the mechanism which produces the welding residual stress and distortion.
(2) It can be used for the measurement of the three dimensional residual stress[11].
(3) Once the inherent strain is known, the residual stress and the distortion can be computed by elastic analysis.
(4) In the assessment of the effect of the welding residual stress and the distortion on the strength and the reliability of structures, inherent strain is an ideal physical value to describe the problem.

3.5 Mechanism of inherent strain production

Since, heat is applied along the line, the thermal cutting, the line heating and the welding are basically the same processes in terms of inherent strain. Only difference is the difference in net heat input per unit length and its distribution on the cross-section. Such differences of heat input make variations in inherent strain, thus in distortions and residual stresses.

The mechanism in which the inherent strain is produced in thermal processes can be explained by using a simple model of a metal bar constrained by an elastic spring as shown in Fig.1. When the bar is heated to Tmax from the room temperature (zero degree) and cooled down to the room temperature, the compressive thermal stress is produced in the heating process as shown in Fig.1. The phenomena change with the value of the maximum temperature Tmax relative to T1 and T2 which are defined as,

$$T_1 = \sigma_Y / \beta \alpha E$$
$$T_2 = 2T_1 \qquad (4)$$

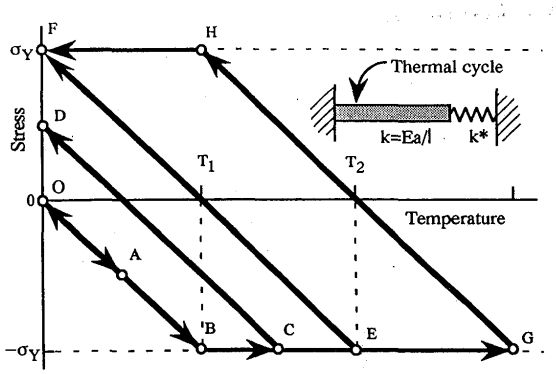

Fig. 1 Stress history of a bar with elastic constraint under thermal cycle.

where, E : Young's modulus
σ_Y : yield stress
α : thermal expansion ratio
β : constraint parameter defined using the stiffnesses of the bar k and the spring k* as in the following equations.

$$\beta=k^*/(k+k^*) \qquad (5)$$

k=aE/L : stiffness of bar
k*: stiffness of spring
a: cross-sectional area of bar
L: length of bar

When $T_{max}<T_1$, the thermal stress does not reach the compressive yield stress in the heating process. Thus, no plastic strain (inherent strain : ε^*) is produced. Since there is no inherent strain, no residual stress nor residual deformation is produced, i.e.

$$\varepsilon^* = 0$$
$$\sigma_R = 0$$
$$\delta_R = 0 \qquad (6)$$

When $T1<T_{max}<T_2$, the thermal stress reaches the yield stress and compressive inherent strain is produced. However, the behavior of the bar is elastic in the cooling process. The inherent strain ε^*, residual stress σ_R and the residual deformation δ_R in this case are,

$$\varepsilon^* = -T_{max}\,\alpha + \varepsilon_Y/\beta = -T_{max}\,\alpha + \sigma_Y/E\beta$$
$$\sigma_R = -\beta E\varepsilon^* = \beta T_{max}\,\alpha\, E - \sigma_Y$$
$$\delta_R = (\varepsilon^* + \varepsilon^e)L = (1-\beta)(-T_{max}\,\alpha + \sigma_Y/E\beta)L \qquad (7)$$

When $T_{max}>T_2$, plastic deformation takes place in both the heating and the cooling processes. The inherent strain ε^*, residual stress σ_R and the residual deformation δ_R in this case are,

$$\varepsilon^* = -\varepsilon_Y/\beta^2 = -\sigma_Y/E\beta^2$$
$$\sigma_R = \sigma_Y$$
$$\delta_R = (\varepsilon^* + \varepsilon^e)L = (1-1/\beta^2)\varepsilon_Y L \qquad (8)$$

As it is seen from Eq.(7) and Eq.(8), the inherent strain is basically determined by both the highest temperature T_{max} and the constraint parameter β.

4. Prediction and Control of Distortion in Assembly Process

4.1 Strategy to tackle problem

For the automation or the introduction of robots in assembly, the precision of parts at each stage of the assembly process, such as cutting, bending and welding, is one of the most important factor to be controlled. To tackle the problem of precision, the following strategy can be proposed.

(1) Precision of the assembly must be considered in the total process including cutting, bending, welding and correction of the distortion.
(2) Identify the most influential factor using FEM simulation
(3) Inherent strain can be used to predict the deformation in cutting and welding.

4.2 Transverse welding deformation in butt weld

The first example is the identification of the influential factors on the transverse welding deformation in butt welding of ship plates[12]. The size of the plate is 8 m by 6 m and the details such as the tack weldings and the tab plates are taken into account as shown in **Fig.2**. From the computations assuming different interval of tack welds and different types of tab plate, the effect of the differences in tack and tab plate is found to be very small as shown in **Fig.3**. Another factor suspected is the geometrical error due to cutting. When large root gap is found, it is closed before

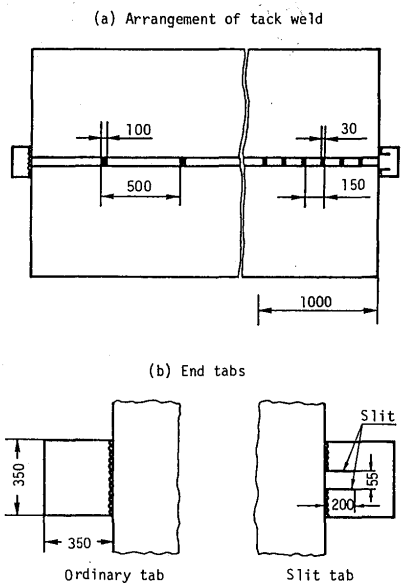

Fig. 2 Types of tack weld and tab plates.

Table 1 Correction method of root gap in butt weld.

Type	Before tack welding	Size of gap	Procedure of correction
Middle -gap	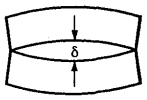	About 5 mm	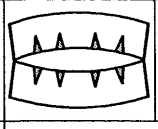 Heat shaded areas. Weld tacks right after gas heating. Close the gap up to about 2-3 mm.
		2-3 mm	Weld tacks from the ends to the middle of the gap. Close the gap up to 1-2mm.
End- gap	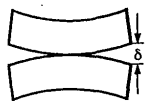	About 5 mm	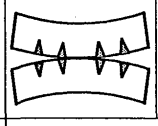 Heat shaded areas. Weld tacks after the plate is cooled down. Close the gap up to about 2-3 mm.
		2-3 mm	Weld tacks from the middle to the ends of the gap. Close the gap up to 1-2mm.
Double -gap	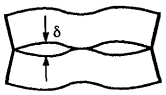		Weld tacks from the place in contact to the middle of gap. Close the gap up to 2-3 mm.

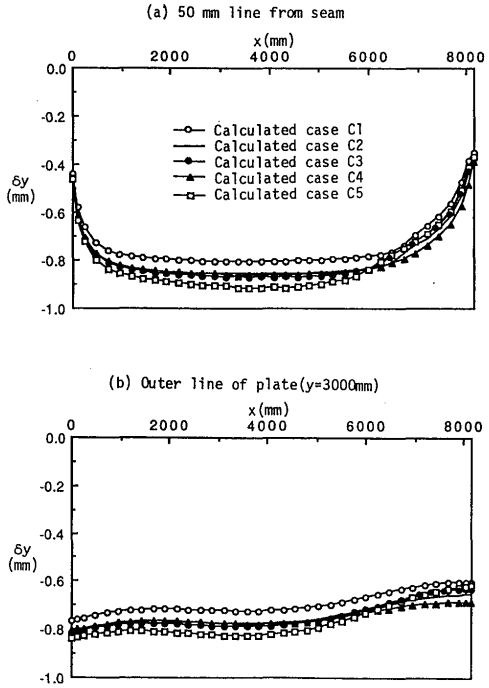

Fig. 3 Effect of tack weld and tab plate types on transverse shrinkage.

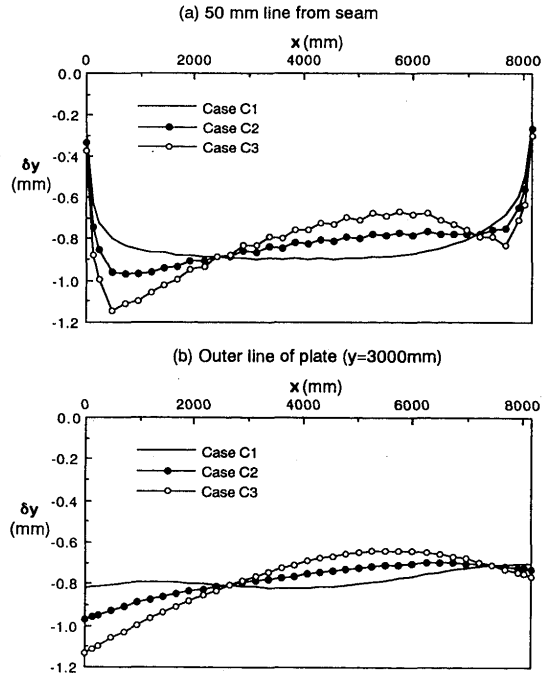

Fig. 4 Transverse shrinkage of welded plate with initial gap.

welding by appropriate methods such as the choice of tack weld sequence or the thermal deformation by gas heating as shown in **Table 1**.

The effect of the initial gap on the welding deformation in the transverse direction is shown by **Fig. 4** [13]. The lines with solid and open circles represent the case with initial gaps of 2 mm and 4 mm at the center, respectively. The simple solid line corresponds to that without the gap. It is seen that the effect of initial gap is very large. This suggests that the accuracy of cutting must be maintained for the better control of the welding deformation.

4.3 Out-of-plane welding deformation in butt weld

The out-of-plane deformation of the

plate due to the butt welding is also analyzed considering the contact between the plate and the working table under the gravitational force[14]. In this study the effectiveness of the constraint by the magnets as shown in **Fig. 5** is examined. The welding deformations with and without the constraint are compared in **Figs. 6** and **7**.

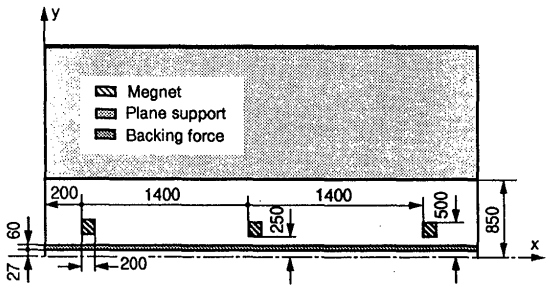

Fig. 5 Arrangements of support, magnet and backing force.

4.4 Geometrical error in thermal cutting

The same thermal-elastic-plastic FEM which is used for the welding problem can be applied to the thermal cutting problems[15]. To clarify the validity of the FEM., the deformation and the residual stress of a plate cut by air-plasma are computed and compared with the measured values in **Figs. 8** and **9**. For both the deformation along the cutting line and the residual stress, the accuracy of FEM is

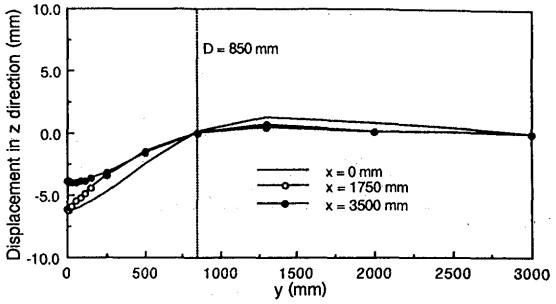

(a) Transverse section

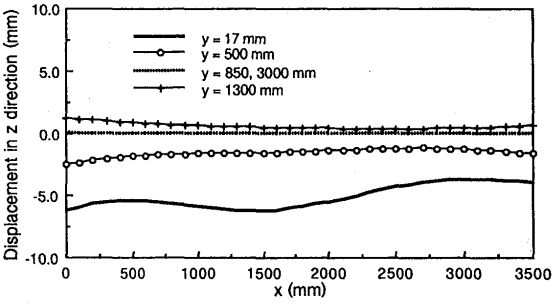

(b) Longitudinal section

Fig. 6 Computed out-of-plane welding deformation (without magnet).

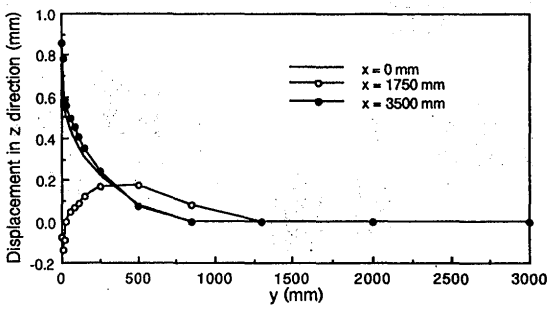

(a) Transverse section

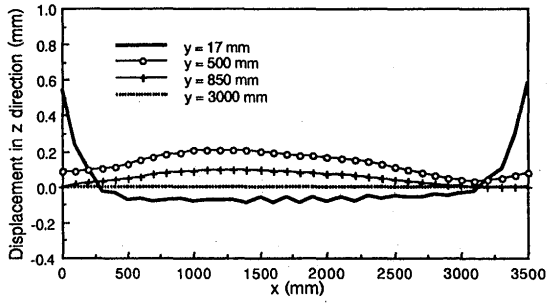

(b) Longitudinal section

Fig. 7 Computed out-of-plane welding deformation (with magnet).

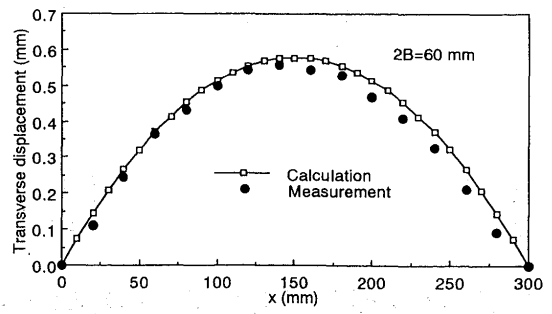

Fig. 8 Computed and measured cutting deformation of thin plate.

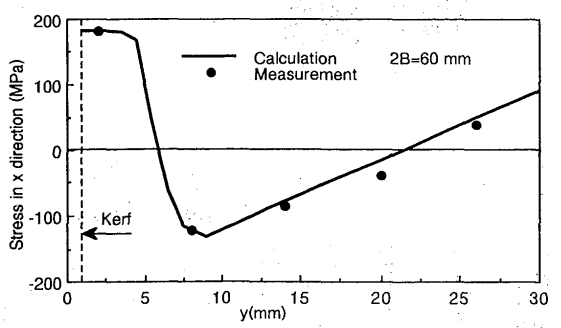

Fig. 9 Computed and measured residual stress due to cutting.

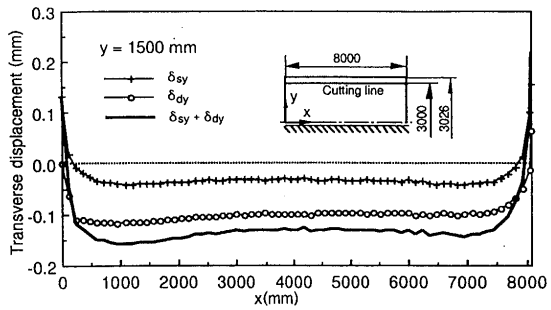

Fig. 10 Distribution of cutting error (two side simultaneous cutting).

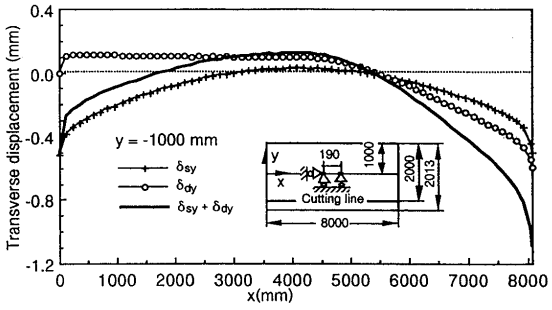

Fig. 11 Distribution of cutting error (one side cutting).

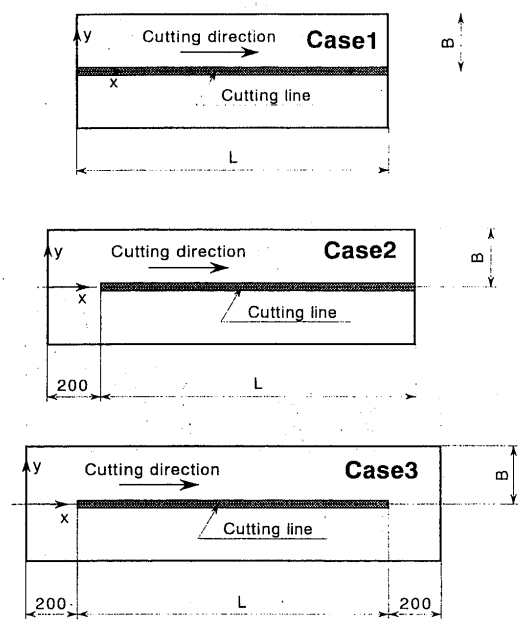

Fig. 12 Models of cutting with different constraint.

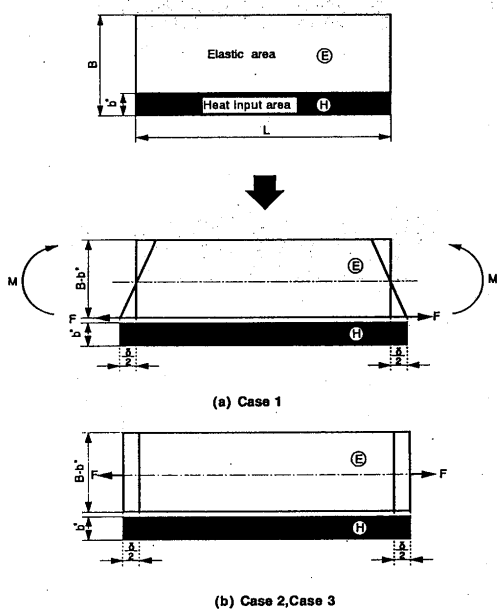

Fig. 13 Simplified constraint model of cutting.

satisfactory. The cutting error can be separated into two parts. One is the deviation of torch from the cutting line due to the transient thermal deformation, δ_{sy}. The other is the deformation caused by the residual plastic strain (inherent strain), δ_{dy}. **Figures 10 and 11** sy are smaller in the two-side simultaneous how that both components of the error δ_{sy} and δ_{dy} are smaller in the two-side simultaneous cutting compared to one-side cutting.

4.5 Inherent strain in thermal cutting

The concept of the inherent strain can be used to study cutting deformation. As it is discussed in chapter 3, the inherent strain produced during the thermal cycle is strongly influenced by the highest temperature and the constraint. **Figure 12** shows three models of cutting specimen with different constraint condition. The strength of the constraint increases in the sequence of Case-1, -2, -3. If the half of the plate with respect to the cutting line is divided into the heated area and the constraining elastic area as shown in **Fig. 13**, the problem can be reduced to the problem of elastically constrained bar discussed in chapter 3. Since the bending deformation is allowed in Case-1, the constraint is small compared to that in Case-2 or -3 in which bending deformation is constrained. Similarly, the constraint becomes larger when the breadth is larger. **Figure 14** shows the effect of the breadth on the inherent strain when the traveling speed of the touch is kept 500 mm/min in Case-1. The solid lines and the broken lines in the figure show the residual plastic strain computed using the thermal-elastic-plastic FEM and that predicted us-

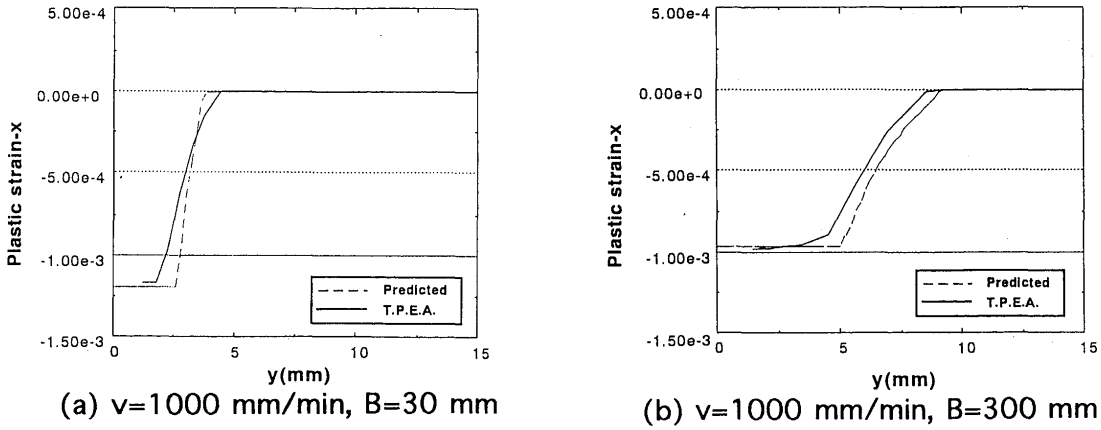

Fig. 14 Effect of plate width on residual plastic strain.

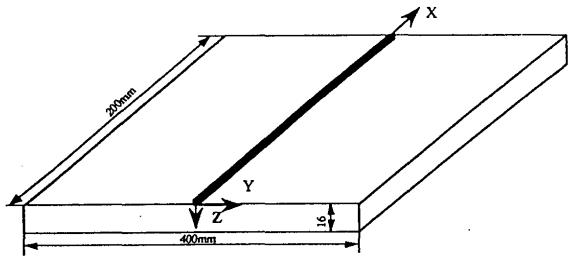

Fig. 15 Bead welding model.

ing a equation derived based on the simple model of a bar with elastic constraint. Since the constraint becomes large as the breadth B increases, the area of inherent strain distribution becomes small, while the value of the inherent strain becomes large when B is large. This can be explained from the general discussion in chapter 3 on T_1 and T_2. The temperatures T_1 and T_2 which determine the distribution area of inherent strain become high if the constraint is small.

4.6 Inherent strain in welding

The fundamental idea involved in the elastically constrained bar can be applied to predict three dimensional distribution of the inherent strain in welding. In case of bead welding as shown in **Fig. 15**, the distribution of the inherent strain is given by the following equations depending on the highest temperature reached at each point[16].

when $T_{max} < T_{1x}$

$$\varepsilon^*_x=\varepsilon^*_y=\varepsilon^*_z=\gamma_{xy}=\gamma_{zx}=\gamma_{yz}=0 \qquad (9)$$

when $T_{1x} < T_{max} < T_{2x}$

$$\varepsilon^*_x=-\alpha T_{max}+\varepsilon_Y/\beta_x$$
$$\varepsilon^*_y=0$$
$$\varepsilon^*_z=-(\varepsilon^*_x+\varepsilon^*_y)$$
$$\gamma_{yz}=0 \qquad (10)$$

when $T_{2x} < T_{max}$

$$\varepsilon^*_x=-\varepsilon_Y/\beta_x$$
$$\varepsilon^*_y=-A\alpha(T_{max}-C)$$
$$\varepsilon^*_z=-(\varepsilon^*_x+\varepsilon^*_y)$$
$$\gamma^*_{yz}=B\alpha(T_{max}-T_{2x})(y/h) \qquad (11)$$

The unknown coefficients in the above formulas are A, B, C and βx. These can be determined using T.E.P. FEM or experiments.

4.7 Comparison between results by T.E.P. and Elastic FEM's

The distribution of inherent strains on the surface at the middle transverse section calculated by the proposed formulas is shown in **Fig. 16**(c). The heat input per unit length Q is assumed to be 800 J/mm in this case. **Figure 17** shows the comparison between the residual stresses computed by the T.E.P. and the Elastic FEM's when Q=1067 J/mm. The transverse shrinkage and the angular distortion computed by the FEM's are compared with the values measured by Satoh et. al[17] in **Figs. 18** and **19**, respectively. As seen from these comparisons, the elastic FEM using the inherent strain determined by the proposed formulas can be used to predict the welding residual stresses and distortions with an acceptable accuracy. **Figure 20** shows the welding deformation of large test model of the ship structure computed using the proposed inherent strain.

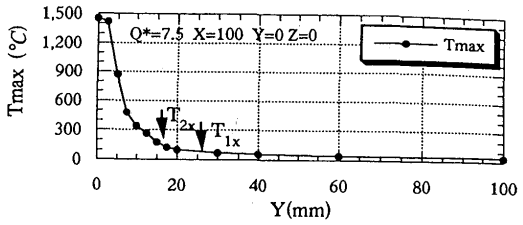

(a) Temperature

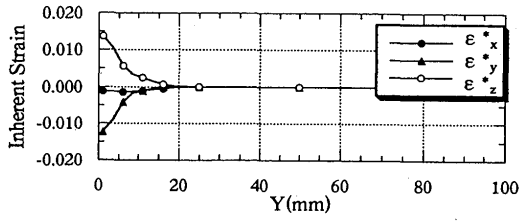

(b) T.E.P

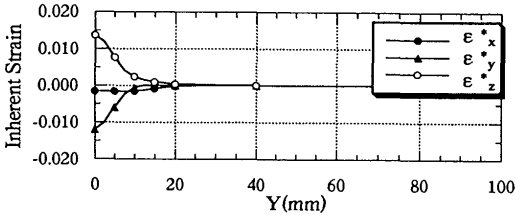

(c) Elastic

Fig. 16 Distribution of highest temperature and inherent strains computed by T.E.P. FEM and proposed formula.

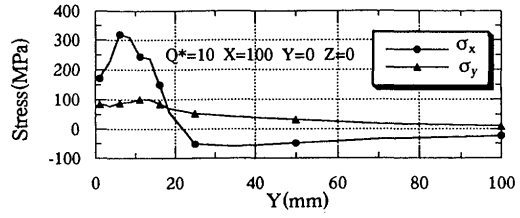

(a) T.E.P

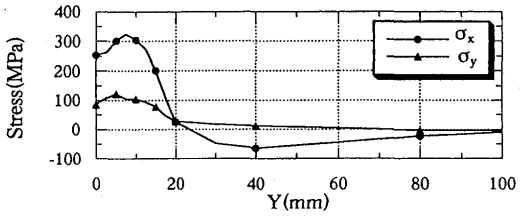

(b) Elastic

Fig. 17 Comparison between stresses computed by T.E.P. and elastic FEM's.

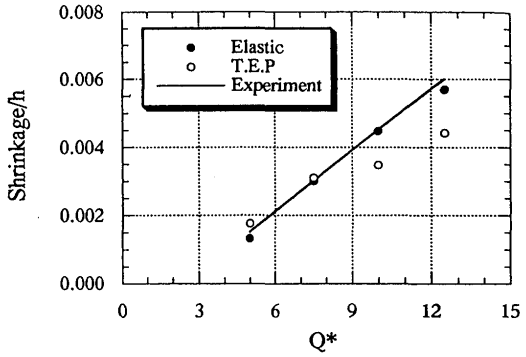

Fig. 18 Transverse shrinkage computed by T.E.P. and elastic FEM's.

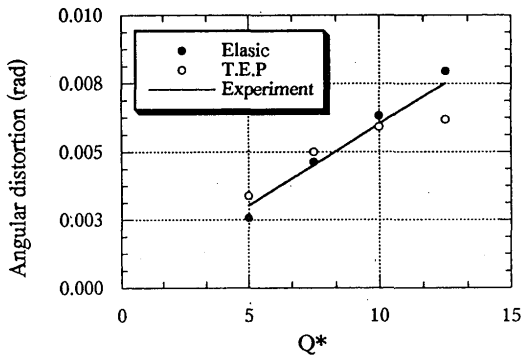

Fig. 19 Angular distortion computed by T.E.P. and elastic FEM's.

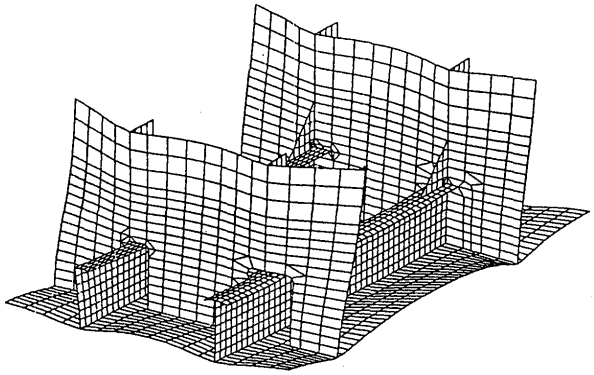

Fig. 20 Welding deformation of large scale test model computed using inherent strain.

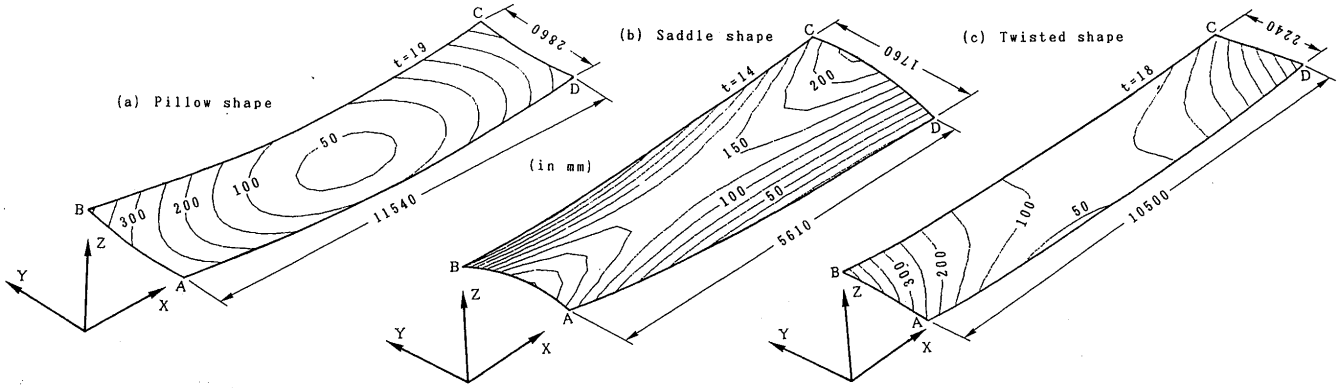

Fig. 21 Typical examples of curved plates in ship structure.

5. Generation of Process Planning for Line Heating

5.1 Characteristics of problem

The FEM and the concept of inherent strain can be also applied to plate bending by line heating. In ship yards in Japan, line-heating or flame bending is widely employed to form curved plate. FEM can be used to predict the deformation caused by the line heating with given heating conditions. If it is used in the inverse manner, instructions on where and how to heat the plate to achieve desired curved shape can be generated[18].

The line heating or the flame bending requires special skill because of the following reasons.

(1) To form a plate, both bending strain and inplane shrinkage are necessary as the inherent strains.
(2) Given inherent strain is turned into the deformation and the residual stress which is invisible.
(3) Plate forming is a geometrically nonlinear problem.
(4) When gas flame is used as a heating device, it is difficult to exactly control the heating condition.

5.2 Strategy to tackle problem

Such a process largely depending on the skill can be a challenging application of computational mechanics. The following strategy was proposed when this research project was started.

(1) The objective is to propose a system for automatic generating of process planning.
(2) To organize the system, the inherent strain is introduced as a fundamental concept.
(3) Since invisible residual stress is difficult to control, inherent strain which does not produce residual stress (compatible strain) must be used for forming.
(4) Compatible inherent strain can be computed by simulating the forced deformation from a flat plate by FEM.
(5) Inherent strain must be separated into the bending and the inplane components.
(6) Ideal heating condition must be selected to create the bending and the inplane inherent strain, respectively.

5.3 Application of computational mechanics

Figure 21 shows three typical shapes of the curved plate for ship hull, namely pillow, saddle and twisted shapes. By analyzing the deformation of a plate from the flat form to the final curved form by FEM, the inherent strains necessary to form the plate is computed. **Figures 22 and 23** show the distribution of the computed bending and inplane strains, respectively. It is seen that the distribution of the bending strain is rather simple. While, the inplane strain shows complex distribution due to its nature of nonlinearlity. Basically, the instruction on where to heat can be generated using these inherent strain distributions. On the other hand, the ideal heating condition for selective generation of the bending or the inplane inherent strain is studied by T.E.P. FEM. According to the similarity, if the temperature field is same, the deformation becomes same. It can be shown that the temperature field is governed by two dimensionless parameters β and ζ

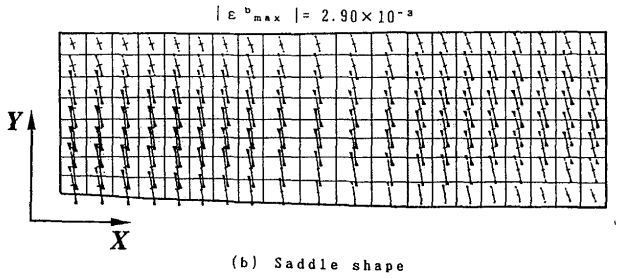

Fig. 22 Distributions of bending inherent strain.

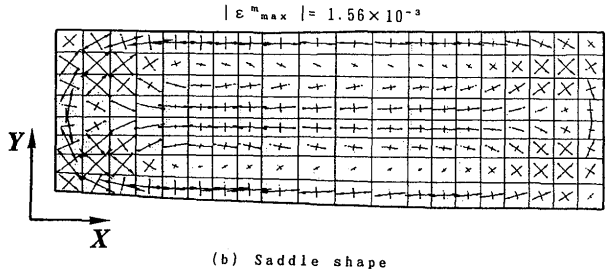

Fig. 23 Distribution of inplane inherent strain.

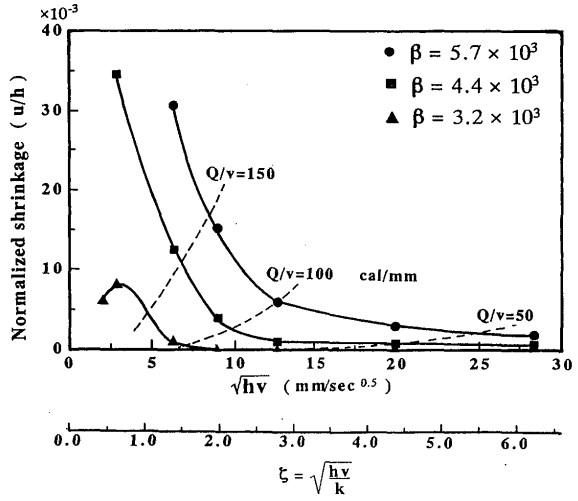

Fig. 24 Relation between transverse shrinkage and parameters β,ξ.

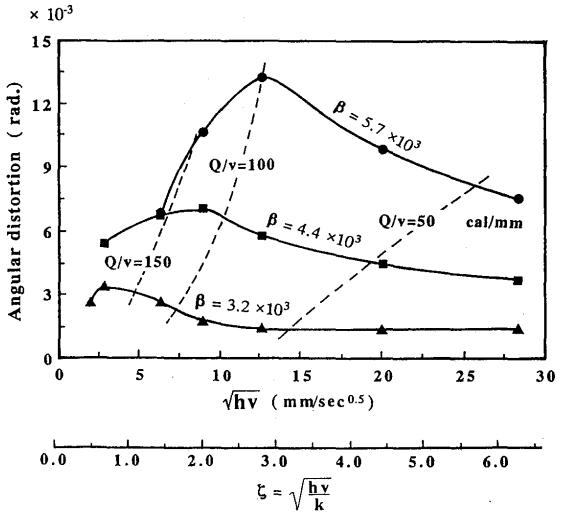

Fig. 25 Relation between angular distortion and parameters β,ξ.

which indicate the maximum surface temperature and the traveling speed of the heat source. The computed value of the bending deformation and the inplane shrinkage are plotted against these parameters in **Figs.24** and **25**. It is clear that there is an ideal point where the maximum bending deformation can be achieved. Using theses figures, ideal heating conditions for generating the bending deformation and the inplane shrinkage can be selected. If the ideal heating condition is not achieved by the conventional gas flame, feasibility of alternative heating method such as induction heating or laser may be tested to innovate the process.

6. Resistance Spot Welding

6.1 Simulation of welding process

Resistance spot welding is slightly different from arc welding. Since the heat is generated by Joule heating, full simulation of the spot welding process including the heat generation is relatively easy. It can be analyzed by FEM[19-22] if the electric field, the thermal field and the displacement field are considered together with the change of contact state, as shown by the flowchart in **Fig.26**. As an example, dome-type and R-type electrodes which are shown in **Fig.27** are considered. **Figures 28** and **29** show the time histories of the highest temperature at the nugget. From these computations, weldability lobes shown in **Figs. 30** and **31** can be drawn. Thus, the performance of the electrodes can be predicted without experiments.

6.2 Application to controlling problem

FEM simulation can be applied to test the controlling method of the power system. In the practical situation, there are various statistical variations. Assuming that the thickness of the plate has variations characterized by the standard variation of 10 %, the

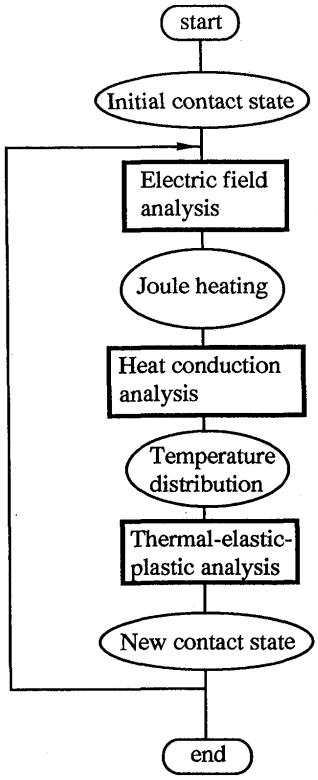

Fig. 26 Flowchart of computation.

effectiveness of the current control is examined using the FEM simulation. Very simple fussy control, in which the current is controlled to achieve ideal time histories of voltage and displacement between the electrodes, is examined. The effectiveness of the control is demonstrated by **Figs.32** and **33** which show the histogram of nugget diameter. It is seen that insufficient nugget size is eliminated by the current control.

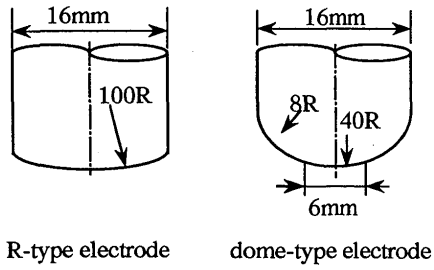

Fig. 27 Two electrodes examined.

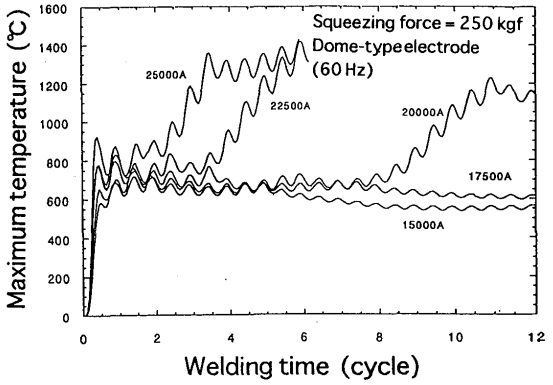

Fig. 28 History of highest temperature in welded zone (dome-type).

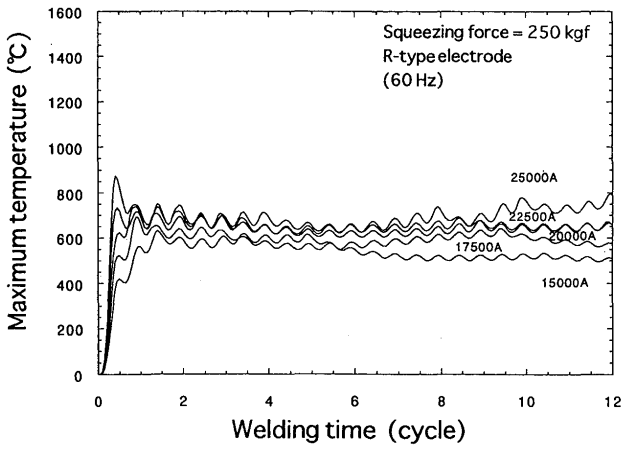

Fig. 29 History of highest temperature in welded zone (R-type).

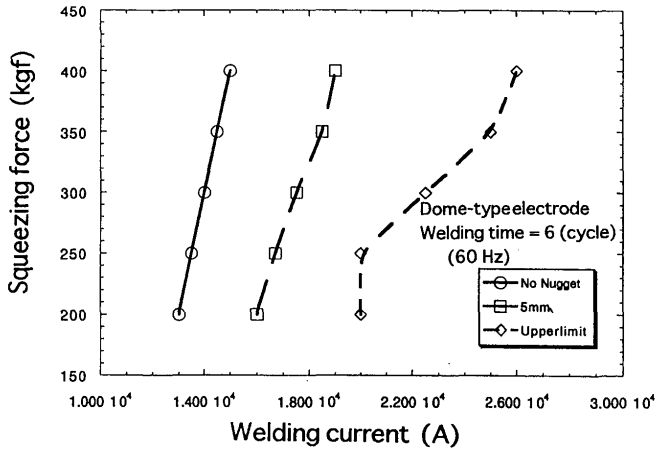

Fig. 30 Weldability lobe for dome-type electrode.

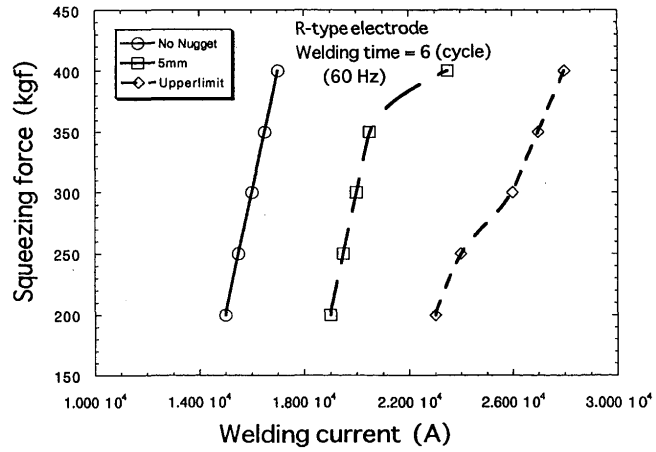

Fig. 31 Weldability lobe for R-type electrode.

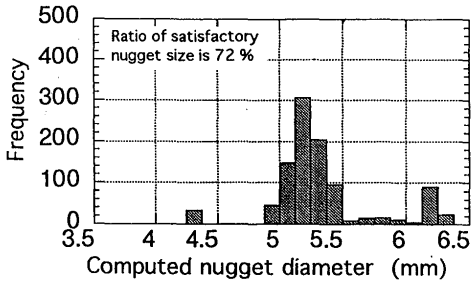

Fig. 32 Histogram of nugget diameter without current control.

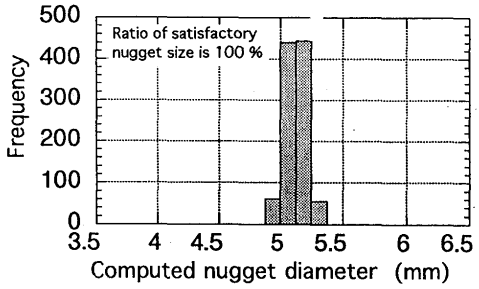

Fig. 33 Histogram of nugget diameter with current control.

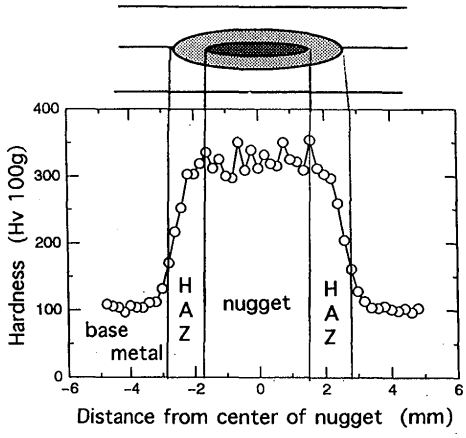

Fig. 34 Measured hardness distribution at weld joint.

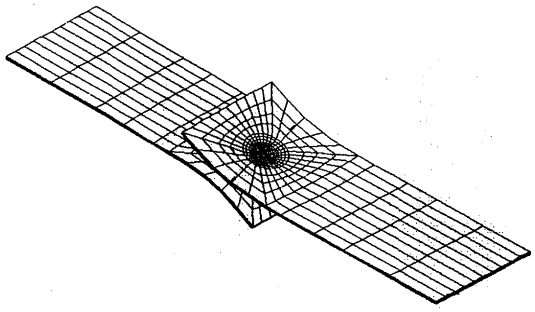

Fig. 35 Computed deformation of joint specimen.

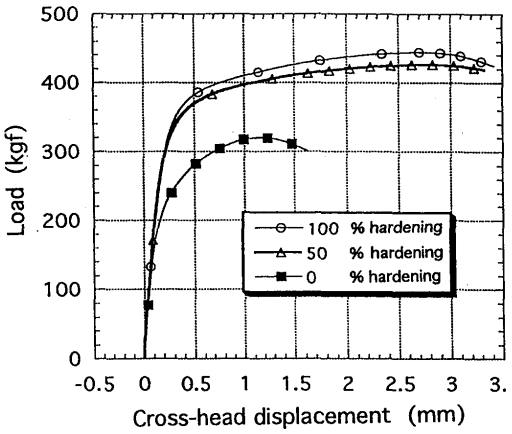

Fig. 36 Effect of hardening on strength of joint.

6.3 Computational mechanics for assessment of strength

If prediction of metallurgical properties such as hardness and fracture toughness are integrated in the simulation, the strength of the weld joint can be predicted. **Figure 34** shows the measured hardness distribution on the cross-section of the weld joint. This measured data is used to examine the influence of the hardening of the heat affected zone (HAZ) on the strength of the joint. The strength is analyses by 3-dimensional FEM assuming large strain elastic-plastic deformation. Computed deformation of the joint is shown in **Fig.35**. The force-displacement curves computed for models with and without hardening are compared in **Fig.36**. It is observed that the hardening of HAZ has a significant contribution on the strength. Though the simulations shown in this chapter involves simplifications and assumptions, they indicate potential usefulness of computational welding mechanics in broad area of application.

7. Conclusion

The computational welding mechanics is not fully established as a science but it is matured enough to be applied to various industrial problems. As mentioned in this report, there is a big gap between the computational welding mechanics and the industrial people. Computational welding mechanics may not be so attractive if it is only the mathematics and computers. The interface is necessary To draw attention of the industry, clear and easily accessed interface is necessary. Such interface can be formed if conceptual modeling and stra-

tegic modeling are integrated with mathematical and numerical modelings. These conceptual and strategic modeling will promote not only practical applications but also further advances of fundamental mathematical and numerical modelings.

References

1)Y. Ueda and T. Yamakawa : Analysis of Thermal Elastic-Plastic Stress and Strain during Welding, IIW Doc. X-616-71(1971), also Trans. Japan Welding Soc., Vol.2 (1971), No.2, 90-100.

2)Y. Fujita and T. Nomoto : Studies on Thermal Elastic-Plastic Problems (1st Report), Journal of the Society of Naval Architects of Japan, Vo.130 (1971), 183-191.

3)N.S. Boulton and H.E. Lance Martin : Proc. Inst. Mech. Engr, 133 (1936), 295-332.

4)J.T. Norton and D. Rosenthal, W.J., 37 (1956).

5)T. Naka and T. Okumura : Thermal Stress Due to Welding on the Thin Steel Plate (part I), J. Welding Soc., Vol.17 (1948), No.3, 2-12 (in Japanese).

6)M. Otani : Graphical Solution of Thermal Stress by Welding (1 st Report), J. Welding Soc., Vol.17 (1948), No.10, 3-12 (in Japanese).

7)M. Watanabe and K. Satoh, Trans. Soc. Naval Architects of Japan, Vol.86 (1954), (in Japanese).

8)I. Tuji : Studies on Elastoplastic Thermal Stresses in Rectangular Plates with Uniaxial Temperature Variation (4th Report) - Transient and Residual Stresses due to butt Welding -, Journal of the Society of Naval Architects of Japan, Vol.118 (1965), 307-317.

9)M. Masubuchi : Stress due to the Distributed Incompatibility, Trans. Soc. Naval Architects of Japan, No.88 (1955), 189-200 (in Japanese).

10)Tsugio Fujimoto : A method for analysis of residual welding stresses and deformations based on the inherent strain, Japan Welding Soc., Vol.39-4 (1970), 236-252 (in Japanese).

11)Y. Ueda, K. Fukuda and M. Tanigawa : A New Measuring Method of Three Dimensional Stress Based on Theory of Inherent Strain, Trans. JWRI, Vol.8 (1979), No.2, 89-96, also Trans. ASME, J. Engineering Materials and Technology, Vol.111 (1989), 1-8.

12)Y. Ueda, H. Murakawa, S. M. Gu, Y. Okumoto and R. Kamichika : Simulation of Welding Deformation for Accurate Ship Assembling (Report I) - In-plane Deformation of Butt Welded Plate -, Trans. Soc. Naval Architects of Japan, No.171 (1992), 335-344 (in Japanese), also Trans. JWRI, 21-2 (1992), 125-135.

13)Y. Ueda, H. Murakawa, Y. Okumoto, S. M. Gu and M. Nakamura : Simulation of Welding Deformation for Accurate Ship Assembling (Report II) - Influence of Initial Imperfection to Butt Welded Plate -, Trans. Soc. Naval Architects of Japan, No.172 (1992), 559 (in Japanese), also Trans. JWRI, 22-1 (1993), 135-144.

14)Y. Ueda, H. Murakawa, S. M. Gu, Y. Okumoto and M. Ishiyama : Simulation of Welding Deformation for Accurate Ship Assembling (Report III) - Out-of-plane Deformation of Butt Welded Plate -, Trans. Soc. Naval Architects of Japan, No.176 (1994), 341-350 (in Japanese), also Trans. JWRI, 25-1 (1996), 69-80.

15)Y. Ueda, H. Murakawa, S. M. Gu, Y. Okumoto and M. Ishiyama : FEM Simulation of Gas and Plasma Cutting with Emphasis on Precision of Cutting, Trans. Soc. Naval Architects of Japan, No.175 (1994), 307-315 (in Japanese), also Trans. JWRI, Vol.23 (1994), No.1, 93-102.

16)Y. Luo, H. Murakawa and Y. Ueda : Prediction of Welding Deformation and Residual Stress by Elastic FEM based on Inherent strain, Proc. of The 6th International Symposium of Japan Welding Society, Nagoya (1996), (to be published).

17)K.Satoh and T. Terasaki : Effect of Welding Conditions on Welding Deformations in Welded Structural Materials, Journal of the Japan Welding Society, Vol.45, No.4(1976), pp.302-308 (in Japanese).

18)Y. Ueda, H. Murakawa, A. M. Rashwan, I. Neki, R. Kamichika, M. Ishiyama and J. Ogawa : Development of Computer Aided Process Planning System for Plate Bending by Line-Heating (Report III) - Relation between Heating Condition and Deformation -, Trans. Soc. Naval Architects of Japan, No.173 (1993), 409-419 (in Japanese), also Trans. JWRI, Vol.22 (1993), No.1, 145-156.

19)H.A. Nied : The Finite Element Modeling of the Resistance Spot Welding Process, Welding Research Supplement, Apr. 1984, pp.123-132.

20)C.L. Tsai, W.L. Dai, D.W. Dickinson and J.C. Papritan : Analysis and Development of a Real-Time Control Methodology in Resistance Spot Welding, Welding Research Supplement, Dec. 1991, pp.339-351.

21)C.L. Tsai, O.A. Jammal, J.C. Papritan and D.W. Dickinson : Modeling of Resistance Spot Weld Nugget Growth, Welding Research Supplement, Feb. 1992, pp.47-54.

22)H. Murakawa, F. Kimura and Y. Ueda : Weldability Analysis of Spot Welding on Aluminum Using FEM, Trans. JWRI, Vol.24 (1995), No.1, 101-111.